STUDIA UBB CHEMIA, LVI, 3, 2011 (p. 27 - 33)

SPECTROSCOPIC EVIDENCE OF COLLAGEN ELECTRODEPOSITION ON ACRYLIC BONE CEMENT

SIMONA CAVALU[a], VIORICA SIMON[b], FLORIN BANICA[a], IOAN OSWALD[a], EMILIA VANEA[b], IPEK AKIN[c], GÜLTEKIN GÖLLER[c]

ABSTRACT. Complementary spectroscopic methods such as FTIR, FT Raman and XPS are applied in this work in order to investigate the surface of acrylic cements after electrolytic deposition of collagen. As an alternative of antibiotic, silver oxide was incorporated in the polymethyl metacrylate (PMMA) matrix and structural properties are discussed by comparing the information obtained using these methods.

Keywords: *collagen, bone cement, ATR FTIR, FT Raman, XPS*

INTRODUCTION

Poly(methyl methacrylate) (PMMA) bone cements are extensively used in certain types of total hip or total knee replacements and are of potential utility wherever mechanical attachments of metal to living bone is necessary [1, 2]. The main function of the cement is to serve as interfacial phase between the high modulus metallic implant and the bone, thereby assisting to transfer and distribute loads [3, 4]. From a chemical point of view, the curing process of the PMMA-based acrylic bone cement, also known as cold curing, is the result of the free radical polymerization of a mixture of PMMA and methyl methacrylate (MMA), initiated by the decomposition of benzoyl peroxide and activated by presence of tertiary amines. During the polymerization process the dough mixture becomes stiff in a short time (10-15 min), which allows the application in situ and the primary fixation of the joint prosthesis. Orthopedic acrylic bone cements have to fulfill several medical requirements, such as low values of maximum cure temperature (to avoid thermal necrosis of the bone tissue during the setting of the cement), moderate sitting time (so that cement does not cure too fast or too slowly), high values of compressive strength (allowing the cured cement mantle to withstand the compressive loads involved by normal daily activities) [5,6,9]. Silver based antimicrobials captured much

---

[a] *University of Oradea, Faculty of Medicine and Pharmacy, P-ta 1Decembrie 10, 410068 Oradea, Romania, scavalu@rdslink.ro*

[b] *Babes-Bolyai University, Faculty of Physics & Institute of Interdisciplinary Research in Bio-Nano-Sciences, Cluj-Napoca, Romania*

[c] *Istanbul Technical University, Metallurgical and Materials Engineering Dept, Istanbul, Turkey*

attention not only because of the non toxicity of the active Ag^+ to human cells [7] but also because of their novelty being a long lasting biocide with high temperature stability and low volatility. The antimicrobial efficacy of these composites depends on their ability to release the silver ions from these composites upon interaction with biological fluids [6]. Hence, silver doped materials are used as an alternative or complementary to antibiotic loaded cements. On the other hand, it has been previously demonstrated that collagen coating increases the proliferation of osteoblasts into the calcium phosphate ceramics [8], as it comprises 90% of the extracellular matrix of bone and occupies a key role in the interaction of osteoblasts and their environment. In the present study, in order to improve the biomineralisation and biocompatibitity of the acrylic bone cement, electrolytic deposition of collagen was performed. The coating was confirmed by different spectroscopic methods: ATR-FTIR, FT-Raman and XPS.

RESULTS AND DISCUSSION

The ATR FTIR spectra recorded before and after collagen electrodeposition on Ag_2O/PMMA bone cement are presented comparatively in Figure 1.

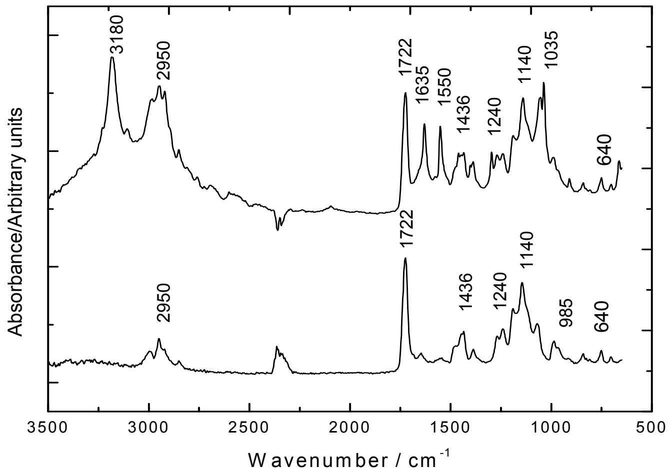

Figure 1. ATR FTIR spectra recorded on the surfaces of the Ag_2O/PMMA before (upper) and after collagen electrodeposition (lower).

The marker bands of PMMA are a sharp and intense peak at 1722 cm^{-1} due to the presence of ester carbonyl group $\nu(C=O)$ stretching vibration, a broad band at 1436 cm^{-1} due to $\delta(CH_3)$ vibration mode, the peaks in the range 1260-1000 cm^{-1} assigned to O-C-O, $C-CH_3$ and C-COO stretching vibrations, and the region between 950-650 cm^{-1} due to the bending of C-H bond [5,10]. In the high wavelength range, the band at 2950 cm^{-1} is due to

CH_2 asymmetric and symmetric stretching, whereas in the low wavelength range, some characteristic bands of Ag_2O are present at 640 and 580 cm^{-1} as an asymmetric O-Ag-O bending mode [11]. The presence of the collagen on the samples surface is confirmed throughout the characteristics of the distinct peaks of collagen: amide I at 1635 cm^{-1} (C=O stretching), amide II at 1550 cm^{-1} (N-H deformation) and amide III around 1200 cm^{-1} (combined N-H bending and C-N stretching). Upon the electrodeposition procedure, the material absorbs a considerable amount of water, as indicated by the large and intense band at 3180 cm^{-1}. In order to obtain complementary information on the surface modifications upon collagen deposition, FT Raman analysis was applied before and after electrodeposition (Figure 2).

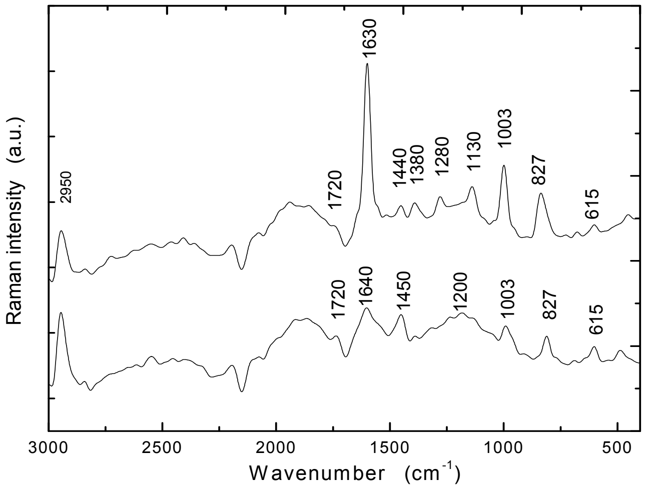

Figure 2. FT Raman spectra recorded on the samples surface before (lower spectrum) and after collagen electrodeposition (upper spectrum).

The main Raman scattering transitions have been observed in PMMA spectra located at 1720 and 1640 cm^{-1}. These transitions are assigned to a stretching mode of the C=O bond in the ester carbonyl group present in both monomer and polymer, and to a stretching mode of the C=C bond present in the monomer only, respectively. According to literature [12,13] the ratio of their intensities should therefore provide a measure of the mass percentage of the uncovered monomer inside the polymer. Other transitions are related to $\delta(CH_3)$ vibration mode at 1450 cm^{-1}, C-O-C stretch vibration at 1003 cm-1, CH_2 rocking vibration at 827 cm^{-1}, while in the low region the bands 615 and 490 cm^{-1} are the Raman vibrations of Ag_2O. Upon collagen deposition, the relative intensities of the Raman bands are strongly modified and shifted. According to the literature [14] the collagen matrix is related to the Raman bands 1650 cm^{-1} (amide I), 1440 cm^{-1} (amide II), and around 1200 cm^{-1} (amide III). In our spectra, the band at 1720 cm^{-1}appears weaker and the band at 1640 cm^{-1} is enhanced and slightly shifted to lower wavenumbers after the electrodeposition procedure. This behavior indicates a reaction between the collagen layer and Ag_2O/PMMA substrate and can be attributed either to hydrogen bonding or to the formation of a new functional group, as the OH deformation band usually appears in the range 1600-1640 cm^{-1}, overlapping the amide I band. If hydrogen bonding occurs, it would involve a weak shift of the carbonyl bond (C=O), making the observation more difficult with Raman spectroscopy. In the IR spectra, frequencies associated with carbonyls (1720 cm^{-1}) are generally not noticeably shifted by hydrogen bonding. In fact, the carbonyl peak is assigned to both non-bonded and H-bonded carbonyls.

The XPS global spectra recorded on the acrylic cement with and without silver oxide, before and after collagen deposition are presented in Figure 3, whereas the core level spectra of nitrogen and silver are showed in Figure 4. The elemental composition on samples surface is presented in Table 1.

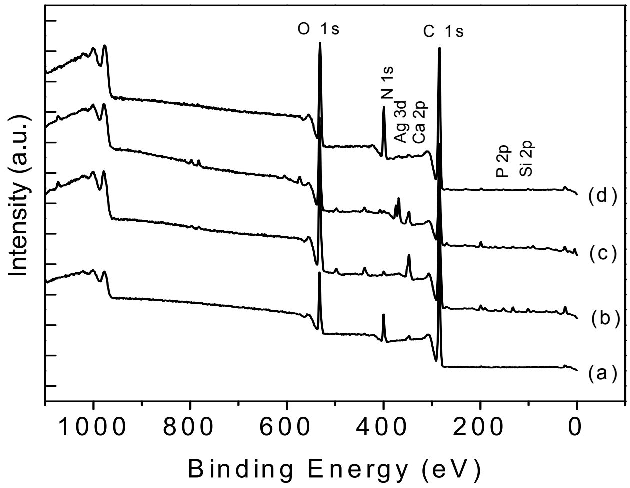

Figure 3. XPS survey spectra of (a) PMMA acrylic cement, (b) PMMA cement after collagen electrodeposition, (c) Ag_2O/PMMA acrylic cement and (d) Ag_2O/PMMA after collagen electrodeposition.

Table 1. Relative percentage of the main components before and after collagen deposition

Sample	**% at**						
	Si	**Ca**	**P**	**Ag**	**O**	**C**	**N**
PMMA	2	3.2	1.9	-	21	70.6	1.3
PMMA/Collagen	0.4	0.7	-	-	12.8	86.1	8.8
Ag_2O/PMMA	0.8	2.2	0.7	1.3	23.2	69.7	2.1
Ag_2O/PMMA/Collagen	0.6	0.3	-	0.1	16.2	70.3	12.5

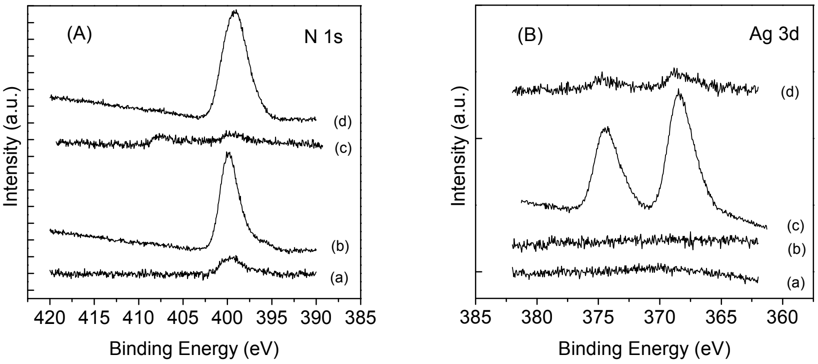

Figure 4. XPS N1s (A) and Ag 3d (B) high resolution spectra of (a) PMMA acrylic cement, (b) PMMA/collagen cement, (c) Ag_2O/PMMA cement and (d) Ag_2O/PMMA/ collagen.

Generally both carbon and nitrogen can be used as markers of proteins attachment due to their presence in great amount in protein structure [15], but as the acrylic cements already contain a significant amount of carbon, in this study only the N 1s will be considered to evaluate collagen deposition. The adsorption of collagen is reflected thus by the evolution of the N 1s photoelectron peak. The nitrogen concentration was very small before protein adsorption and considerably increases especially for the silver containing acrylic cement. The N 1s core level spectra (Figure 4A) reveals a peak at 400 eV, characteristic to C-NH_2 groups [16]. On the other hand, due to the protein coverage, a significant reduction of Ag 3d photoelectron peaks (Figure 4B) is observed. The composition of the samples surface with respect to Si, Ca, P and Ag (Table 1) is also modified compared with that recorded before collagen deposition, being another proof of collagen surface coverage. At the same time, the amount of oxygen decreases for both collagen coated samples (with or without silver oxide) due to the fact that collagen is less rich in oxygen atoms comparing the substrate used. The results show that the silver oxide presence in PMMA matrix improves the protein attachment, and, according to the literature, Ag^+ reacts with thiol groups in proteins, due to a high affinity between sulphide and the soft metal [17, 18].

CONCLUSIONS

The surface of Ag_2O/PMMA acrylic bone cement was investigated by complementary FTIR, FT Raman and XPS spectroscopy before and after collagen electrodeposition. The results confirm the presence and stability of the collagen layer on the surface. Moreover, they indicate that silver oxide presence in PMMA matrix improves the protein attachment.

EXPERIMENTAL SECTION

The investigated materials were prepared using commercial PMMA based cements as starting material (Biomecanica Ind. Brasil), having the following composition: liquid- methylmethacrylate (monomer) 84.4%, butylmethacrylate 13.2%, N:N dimethyl p- toluidine 2.4%, hidroquinone 20 ppm; powder - methylmethacrylate (copolymer) 87.3%, polymethyl metacrylate 2.7 %, barium sulphate 10%. As antimicrobial agent, Ag_2O particles were incorporated with respect to the total powder amount in a concentration of 5 %(w/w). Electrolytic deposition of soluble collagen type I from calf skin (Fluka) was carried out in a three-electrode electrochemistry system working in chronoamperometric mode, as previously reported [9]. The sample surfaces were analyzed by complementary FTIR, FT Raman and XPS spectroscopy. The equipments used were Spectrum BX Perkin Elmer FTIR spectrometer, equipped with MIRacle ATR accessory (ZnSe crystal), spectra collected in the wavelength range 4000-400 cm^{-1} at a nominal resolution of 4 cm^{-1}, with a scanning speed of 32 cm^{-1}, total 100 scans being accumulated for each spectrum; FT Raman Bruker EQUINOX 55 equipment, spectra collected at 4 cm^{-1} resolution, with 600 scans and laser power between 100-370 mW; SPECS PHOIBOS 150 MCD system equipped with monochromatic Al-K_α source (250 W, hv=1486.6 eV), hemispherical analyser and multichannel detector;the typical vacuum in the analysis chamber during the measurements was in the range of 10^{-9}- 10^{-10} mBar and the binding energy scale was charge referenced to the C 1s at 284.6 eV. The samples surfaces were analysed before and after collagen electrodeposition.

ACKNOWLEDGMENTS

This study was accomplished in the framework of Romanian-Turkey Bilateral Cooperation project 385/2010.

REFERENCES

1. J. Charnley, “Acrylic Cement in Orthopaedic Surgery” Williams and Wilkins Eds, Baltimore, USA, **1970,** chapter 1.
2. S. J. Breusch, K.-D. Kuhn, *Orthopade,* **2003**, *32*, 41.
3. F. R. DiMaio, *Orthopaedics*, **2002,** *25*, 1399.
4. W. R. Krause, “Encyclopedia of Medical Devices and Instrumentations”, J. G. Webster (ed), Willey, New York, USA, **1988,** vol.1.
5. S. Cavalu, V. Simon, *Journal of Optoelectronics and Applied Materials,* **2006,** *8/4*, 1520.

6. S. Cavalu, V. Simon, G. Goller, I. Akin, *Digest Lournal of Nanomaterials and Biostructructures*, **2011** *6/2*, 779.
7. J. Hardes, A. Streitburger, H. Ahrens, T. Nusselt, C. Gebert, W. Winkelmann, A. Battmann, G. Gosheger, *Sarcoma*, **2007**, art. no. 26539.
8. Y. Fan, K. Duan, R. Wang, *Biomaterials* , **2005**, *26,* 1623.
9. S. Cavalu, V. Simon, F. Banica, *Digest Lournal of Nanomaterials and Biostructructures*, **2011***, 6/1,* 89.
10. A. Balamurugan, S. Kannan, V. Selvaraj, S. Rajeswari, *Trends in Biomaterials and Artificial Organs,* **2004**, *18*, 41.
11. G. I. N. Waterhouse, G. A. Bowmaker, J. B. Metson, *Physical Chemistry Physics*, **2001**, *3*, 3838.
12. F. Pallikari, G. Chondrokoukis, M. Rebelakis, Y. Kotsalas, *Materials Research and Innovations*, **2001**, *4,* 89.
13. C.P. Hagan, J.F. Orr, C.A. Mitchell, N.J. Dune, *Journal of Materials Science: Materials in Medicine*, **2009,** *20*, 2427.
14. J. Xu, I. Stangel, I.S. Butler, D.F.R. Gilson, *Journal of Dental Research*, **1997**, *76*, 596.
15. E. Vanea, V. Simon, *Applied Surface Science,* **2011**, *257*, 2346.
16. M. Advincula, X. Fan, L. Lemons, R. Advincula, *Colloid Surface B*, **2005**, *42*, 29.
17. A. Simchi, E. Tamjid, F. Pishbin, A.R. Boccaccini, *Nanomedicine : nanotechnology, biology, and medicine*, **2011,** *7,* 22.
18. Q.L. Feng, J. Wu, G.Q. Chen, F.Z. Cui, T.N. Kim, J.O. Kim, *Journal of Biomedical Materials Research,* **2000**, *52*, 662.